



OPEN

Agriculture increases the bioavailability of silicon, a beneficial element for crop, in temperate soils

M. Caubet¹, S. Cornu²✉, N. P. A. Saby¹ & J.-D. Meunier²

Crops may take benefits from silicon (Si) uptake in soil. Plant available Si (PAS) can be affected by natural weathering processes or by anthropogenic forces such as agriculture. The soil parameters that control the pool of PAS are still poorly documented, particularly in temperate climates. In this study, we documented PAS in France, based on statistical analysis of Si extracted by CaCl₂ (Si_{CaCl2}) and topsoil characteristics from an extensive dataset. We showed that cultivation increased Si_{CaCl2} for soils developed on sediments, that cover 73% of France. This increase is due to liming for non-carbonated soils on sediments that are slightly acidic to acidic when non-cultivated. The analysis performed on non-cultivated soils confirmed that Si_{CaCl2} increased with the < 2 μm fraction and pH but only for soils with a < 2 μm fraction ranging from 50 to 325 g kg⁻¹. This increase may be explained by the < 2 μm fraction mineralogy, i.e. nature of the clay minerals and iron oxide content. Finally, we suggest that 4% of French soils used for wheat cultivation could be deficient in Si_{CaCl2}.

Silicon (Si) has been shown to be beneficial for crops exposed to biotic or abiotic stresses^{1–5}. The role of Si remains controversial^{1,6}, but crop yields may depend on the bioavailable Si in the soil⁷, particularly for globally cultivated crops and staple food that contain 1% or more Si by dry weight such as rice, sugar cane, or wheat, or more broadly, the Poaceae^{8–10}. Soil Si bioavailability is therefore an emerging issue in agriculture, as Si fertilization of soil depleted of bioavailable Si could increase yields^{8,11–13}.

Si is taken up from the soil solution by roots and is accumulated in the shoots in the form of amorphous silica particles (phytoliths). In the soil solution, dissolved Si (DSi) primarily occurs in the neutral form Si(OH)₄ (silicic acid). The DSi concentration typically ranges from 0.1 to 0.6 mmol L⁻¹¹³. DSi originates from the dissolution of primary and secondary silicate minerals through alteration or chemical weathering¹⁴ and from plant recycling through the dissolution of phytoliths^{15,16}. The alterability of silicate minerals can be characterized by their solubility and kinetic properties, which are dependent upon temperature, pH, and available solutes^{17,18}.

DSi concentration in the soil solution can be lowered by plant uptake¹⁹, uptake by silica-shelled microorganisms²⁰ and Si adsorption to mineral surfaces²¹. Quantifying the pool of Si that is bioavailable (PAS) is still a challenge⁷. Si extracted with CaCl₂ (Si_{CaCl2}), acetate, acetic acid, or citrate are used as PAS proxies since the concentrations extracted by these reagents are proportional to plant Si concentration or grain yield^{22,23}. PAS concentrations extracted by these reagents have been shown to be positively correlated with soil properties such as phytolith content²⁴, pH^{25–27}, < 2 μm fraction^{7,28}, organic matter, and iron oxides²⁸. A negative correlation between PAS and total Si content has also been documented, reflecting the predominance of low solubility minerals such as quartz in the Si pool^{28,29}. Critical levels of PAS have been identified in cultivated lands mainly under tropical climate including the paddy soils of Asia^{7,30}, the USA³¹, and Brazil³², and the sugarcane fields of Australia³³. Under critical levels of PAS, silicate fertilization may be recommended and is already applied on tropical soils in some countries.

Chemical weathering leads to a removal of Si through leaching and erosion¹⁴. Intense weathering causes soils to become acidic and depleted in bases and Si (desilication) due to loss of primary silicates that are easily weatherable. Cultivation, through exportation of crops containing silicon has been indicated as a Si pool modifier by lowering the phytolith pool^{34–39}; as a consequence, cultivation may reduce the soil Si availability if plant residues are not returned to the fields⁴⁰. Darmawan et al.¹¹ documented a significant decrease of available Si after approximately 30 years of intensive rice cultivation in Indonesia. The decrease of PAS in soil has been listed as a

¹INRAE, Infosol, US 1106, Orléans, France. ²Aix-Marseille Univ, CNRS, IRD, Coll de France, INRAE, CEREGE, Aix-en-Provence, France. ✉email: sophie.cornu@inrae.fr

Soil parent material/type	Land use	Si _{CaCl2} (mg kg ⁻¹)					n
		Mean	Sd	Q25	Q50	Q75	
Carbonated soils on sediment	All	31	17	20	26 ^a	36	516
	Non-cultivated	25	11	17	23	30	219
	Cultivated	35	20	23	29	41	297
Soils on igneous extrusive rock	All	51	27	32	47 ^b	66	29
Soils on igneous intrusive rock	All	11	5.7	8.6	10 ^c	13	155
	Non-cultivated	12	6.1	8.8	11	14	109
	Cultivated	10	4.2	7.6	9.3	11	46
Soils on metamorphic rock	All	11	5.8	7.8	9.6 ^c	13	217
	Non-cultivated	11	5.8	7.5	9.5	13	120
	Cultivated	12	5.9	8.1	9.7	14	97
Non-carbonated soils on sediment	All	20	15	9.2	16 ^d	28	1013
	Non-cultivated	16	13	7.9	12	21	537
	Cultivated	25	16	12	23	34	476
Podzols	All	5.1	2.8	3.7	4.2 ^e	4.9	56
All data (<i>subset 1</i>)		21	16	9.5	17	28	1986

Table 1. Summary statistics of Si_{CaCl2} concentrations measured for the *subset 1* (Supplementary Table S1). The summary statistics are provided for the combination of a parent material group and land use. Q25, Q50, and Q75 are the 25%, 50%, and 75% percentile, respectively. Medians sharing a letter are not significantly different according to pairwise comparisons of Wilcoxon test with Tukey adjustment for multiple comparisons.

factor contributing to the stagnation of crop yields¹². Si supply is considered a useful strategy for improving crop health⁷, the influence of land use and agricultural practices on PAS has become an emerging issue⁴¹.

The objectives of this paper are to determine the impact of agriculture on PAS in temperate soils. To do so we (i) estimated the spatial variability of PAS in France, a country with a high soil diversity⁴² that can be considered as representative of most European soils, and likely be of most temperate soils worldwide; (ii) hierarchized the soil characteristics governing this variability in non-cultivated soils for different soil groups (pH, < 2 μm fraction, cation exchange capacity (CEC), major elements) to (iii) understand how and under which pedological conditions, cultivation acts on these soil divers; and (iv) determine which soils may exhibit too low Si_{CaCl2} concentrations in soil solution for proper growth of wheat, a Si accumulator plant.

We implemented a spatial statistical approach based on an extensive dataset extracted from the French Soil Quality Monitoring Network database⁴³. This dataset contains data from over 2200 sites in the France mainland, all of which were analysed for major chemical, physical, pedological, climatic, and geological parameters including Si_{CaCl2} concentrations. We focused on the Si_{CaCl2} soil concentrations of the surface horizons (0–30 cm), considered to be the horizon most explored by plant roots.

Results and discussion

Variables explaining Si_{CaCl2} using digital soil mapping (DSM). Concentrations of Si_{CaCl2} in French topsoils ranged from 2.3 to 134 mg kg⁻¹ (*subset 1*, see Supplementary Table S1) with a 1st quartile value of 9.5 mg kg⁻¹, a median of 17 mg kg⁻¹, and a 3rd quartile of 28 mg kg⁻¹ (Table 1). The values fell in the same range as values found elsewhere^{25,26}.

The spatial distribution of Si_{CaCl2} at the French territory scale obtained by the DSM approach was evaluated by the following criteria using a 30-fold cross validation process: R² = 0.43, concordance = 0.58, RMSE = 13 mg kg⁻¹, and bias = 0.24 mg kg⁻¹. These criteria are of the same order of magnitude than those obtained in other DSM studies, at national scale, for other soil parameters, which yield R² ranging from 0.25 to 0.55^{44–46}. The most important covariates for predicting the spatial pattern of the Si_{CaCl2} concentration in the obtained Random Forest model, was, as expected, the parent material (*parent_material*) (Fig. 1). The second most important covariate was the so called *NDVI_1*, a proxy for vegetation growth dynamics as defined by Loiseau et al.⁴⁷. Other important covariates for the model were soil type, precipitation, and land use, in that order. These results confirmed the data obtained in Japan²⁸ and in Louisiana³¹ indicating that PAS depends on pedological/geological conditions. As a consequence, the primary spatial structures of the map (Fig. 2a) matched the parent materials and the negative correlation with total Si concentration²⁹. These results also highlighted the importance of land use/vegetation on the Si_{CaCl2} concentration.

Physical and chemical control of Si_{CaCl2} in non-cultivated soils. In this part, only non-cultivated soils are considered to study the mechanisms that occur naturally in soils, without the influence of agriculture that generally strongly modifies some of the soil characteristics considered as PAS drivers, notably the soil pH by liming for slightly acidic to acidic soils, the soil organic carbon concentration (SOC).

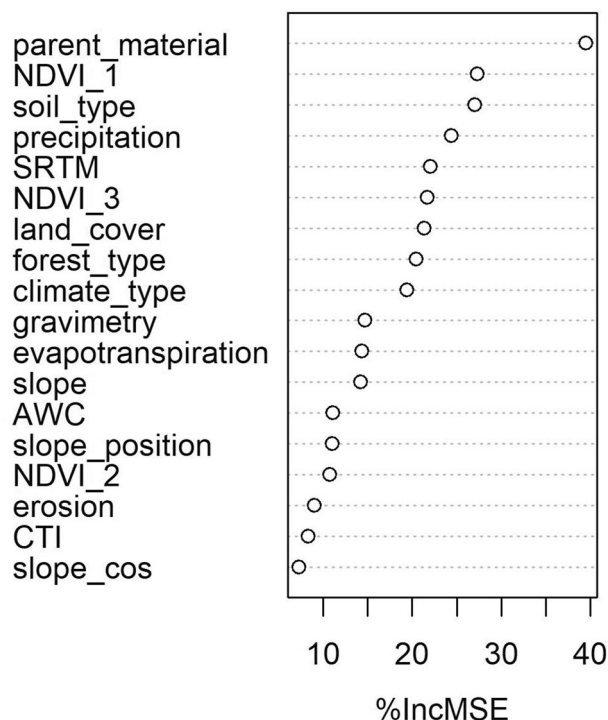


Figure 1. Importance of variables in the Random Forest model (in % of increasing Mean Squared Error, %IncMSE).

Overall correlations between the main soil characteristics and Si_{CaCl_2} concentrations. In the non-cultivated soils, we confirmed previous findings indicating that Si_{CaCl_2} concentration was positively correlated (Table 2) with pH ($r=0.46$) and the $<2\ \mu m$ fraction ($r=0.59$). The relationships with SOC and iron oxides (estimated by the Mehra Jackson extraction method⁴⁸) were weaker (with r of 0.27 and 0.35, respectively). Si_{CaCl_2} was also positively correlated with CEC ($r=0.59$), exchangeable Ca ($r=0.54$), and CEC of $<2\ \mu m$ fraction ($r=0.44$). The correlation of Si_{CaCl_2} with pH indicated that Si_{CaCl_2} concentration may be controlled by Si adsorbed on the surface of soil minerals and/or by the soil weathering state^{25,26}. The correlation of Si_{CaCl_2} with the $<2\ \mu m$ fraction can be attributed to the presence of small phytoliths⁴⁹, clay mineral dissolution⁵⁰, or adsorption onto clay minerals⁵¹.

Nevertheless, while Si_{CaCl_2} linearly increased with the $<2\ \mu m$ fraction in non-cultivated soils regardless of parent material (Fig. 3a), the correlation with pH was more complex. The concentration in Si_{CaCl_2} increases with pH for pH values lower than 6–7 and then slightly decreases for pH larger than 8 (Fig. 3b). Such an evolution of Si_{CaCl_2} with pH was already described in the literature⁵². As a consequence, there was no correlation between Si_{CaCl_2} and the soil pH (Table 2) for carbonated soils due to their high (>7) and rather constant pH values (Fig. 4b). For the SOC and Fe oxides, the relationship with Si_{CaCl_2} is less marked, even though the Si_{CaCl_2} concentration globally increases with these parameters (Fig. 3c,d). As a conclusion, in non-cultivated soils, the Si_{CaCl_2} concentration seems to be mainly driven by $<2\ \mu m$ content and pH suggesting adsorption.

The impact of pH on the Si_{CaCl_2} concentration is a function of the $<2\ \mu m$ fraction. To explore the respective role of pH, CEC of $<2\ \mu m$ fraction, and $<2\ \mu m$ fraction on Si_{CaCl_2} concentrations in soils, we considered the correlation between soil Si_{CaCl_2} concentration and soil pH for each of the $<2\ \mu m$ fractions defined in Fig. 3a. For low $<2\ \mu m$ fraction concentrations ($<50\ g\ kg^{-1}$), the Si_{CaCl_2} concentration was significantly correlated with the pH but the slope of the regression was very low and appeared to be driven by a few extreme values (Fig. 5). As a result, Si_{CaCl_2} concentrations increased minimally from 3.3–4.3 $mg\ kg^{-1}$ to 6.4–9.3 $mg\ kg^{-1}$ in 4.5 pH units, demonstrating the low impact of pH on Si_{CaCl_2} concentration for soils with poor $<2\ \mu m$ fractions. For $<2\ \mu m$ fraction concentrations ranging from 50 to 325 $g\ kg^{-1}$, Si_{CaCl_2} concentration increased with pH. Nevertheless, for $<2\ \mu m$ fraction content higher than 230 $g\ kg^{-1}$, the increase of Si_{CaCl_2} with pH is smaller. No correlation is observed for $<2\ \mu m$ fraction concentrations higher than 325 $g\ kg^{-1}$, indicating that adsorption might not be the dominant process at these $<2\ \mu m$ contents. Carbonated soils are in this $<2\ \mu m$ fraction range (median of 364 $g\ kg^{-1}$, Supplementary Table S2) explaining the absence of correlation of Si_{CaCl_2} with pH.

As a conclusion, the classically described increase of Si_{CaCl_2} with pH (explained by Si adsorption processes) was only encountered in temperate soils for non-carbonated soils with $<2\ \mu m$ concentrations higher than 50 $g\ kg^{-1}$ or lower than 325 $g\ kg^{-1}$.

Impact of the nature of the $<2\ \mu m$ fraction on Si_{CaCl_2} concentration. The $<2\ \mu m$ CEC can be used as a proxy for the nature of the clay minerals of the soil as shown by the contrasted CEC of the different clay minerals provided by Goldberg et al.⁵³. On this basis⁵³, we assumed that (i) soils with $<2\ \mu m$ CEC lower than 10 $cmol^+\ kg^{-1}$ were

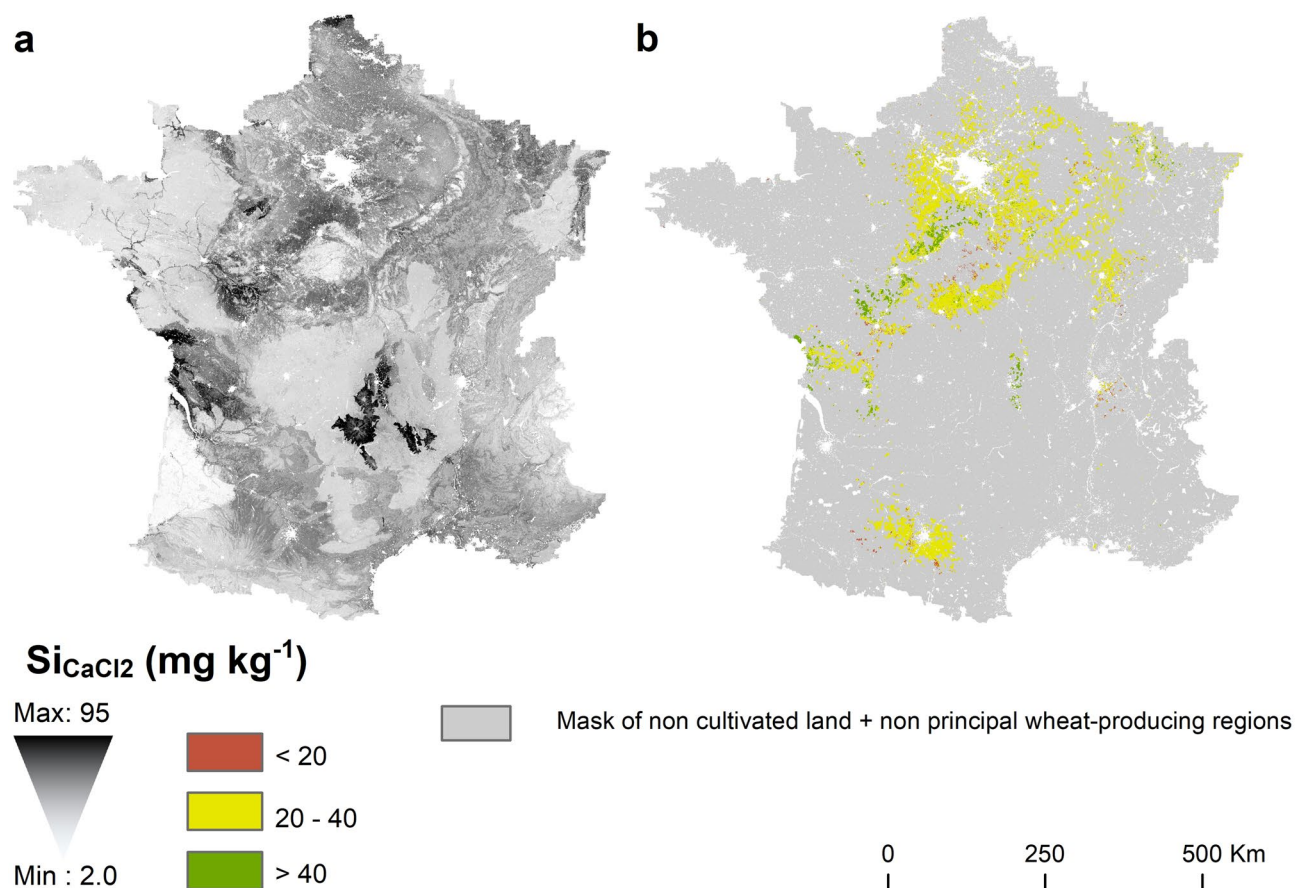


Figure 2. Regression Kriging predictions of $\text{Si}_{\text{CaCl}_2}$ concentrations in French topsoils at 90 m resolution. (a) continuous colour gradient representation; (b) categorical representation in 3 classes of $\text{Si}_{\text{CaCl}_2}$ concentrations based on critical values defined for sugarcane and rice^{28,29,31} for soils cropped in wheat, obtained by crossing the 'arable land' pixels, 'permanent crop' and 'heterogeneous agricultural' areas with the exception of 'agro-forestry' of Corine Land Cover classes⁵⁴ with municipalities for which type of farming is primarily cereal crop, according to French OTEX classification (Orientation Technico-Economique des Exploitations). We removed the municipalities from 7 departments (Ain, Haut-Rhin, Bas-Rhin, Gironde, Pyrénées-Atlantiques, Hautes Pyrénées, Landes) where corn is the main cereal under production. Maps were generated using ArcGIS software version 10.7.1 (ESRI: <https://www.esri.com/en-us/home>).

Class	$\text{Si}_{\text{CaCl}_2} \sim \text{pH}$	$\text{Si}_{\text{CaCl}_2} \sim (<2 \mu\text{m fraction})$	$\text{Si}_{\text{CaCl}_2} \sim (<2 \mu\text{m CEC})$	n
All non-cultivated soils	0.46	0.59	0.44	1065
Carbonated soils on sediment	- 0.099	0.2	0.093	219
Soils on igneous extrusive rock	0.63	0.66	0.63	27
Soils on igneous intrusive rock	0.25	0.39	0.36	109
Soils on metamorphic rock	0.3	0.42	0.3	120
Non-carbonated soils on sediment	0.48	0.68	0.48	537
Podzols	0.034	0.81	0.15	53

Table 2. Correlation coefficients between $\text{Si}_{\text{CaCl}_2}$ and pH, $<2 \mu\text{m}$, and CEC of the $<2 \mu\text{m}$ fraction ($<2 \mu\text{m}$ CEC) for the non-agricultural soils as a whole and by classes of parent material. Significant correlations (p value < 0.05) are reported in bold. Medians sharing a letter are not significantly different according to pairwise comparisons of Wilcoxon test with Tukey adjustment for multiple comparisons.

primarily kaolinitic or possessed a $<2 \mu\text{m}$ fraction rich in quartz; (ii) soils with $<2 \mu\text{m}$ CEC ranging from 10 to $40 \text{ cmol}^+ \text{ kg}^{-1}$ contained a large amount of illite and chlorite or a complex mixture of clay minerals; and (iii) soils with a $<2 \mu\text{m}$ CEC larger than $40 \text{ cmol}^+ \text{ kg}^{-1}$ contained a large quantity of vermiculite and smectite.

A correlation of the $\text{Si}_{\text{CaCl}_2}$ concentrations with the $<2 \mu\text{m}$ CEC (a proxy for the nature of the clay minerals of the soil) was observed globally and for all non-carbonated parent material, with the exception of podzols (Table 2), suggesting a role of the nature of the clay minerals on the $\text{Si}_{\text{CaCl}_2}$ concentrations. However, Fig. 5

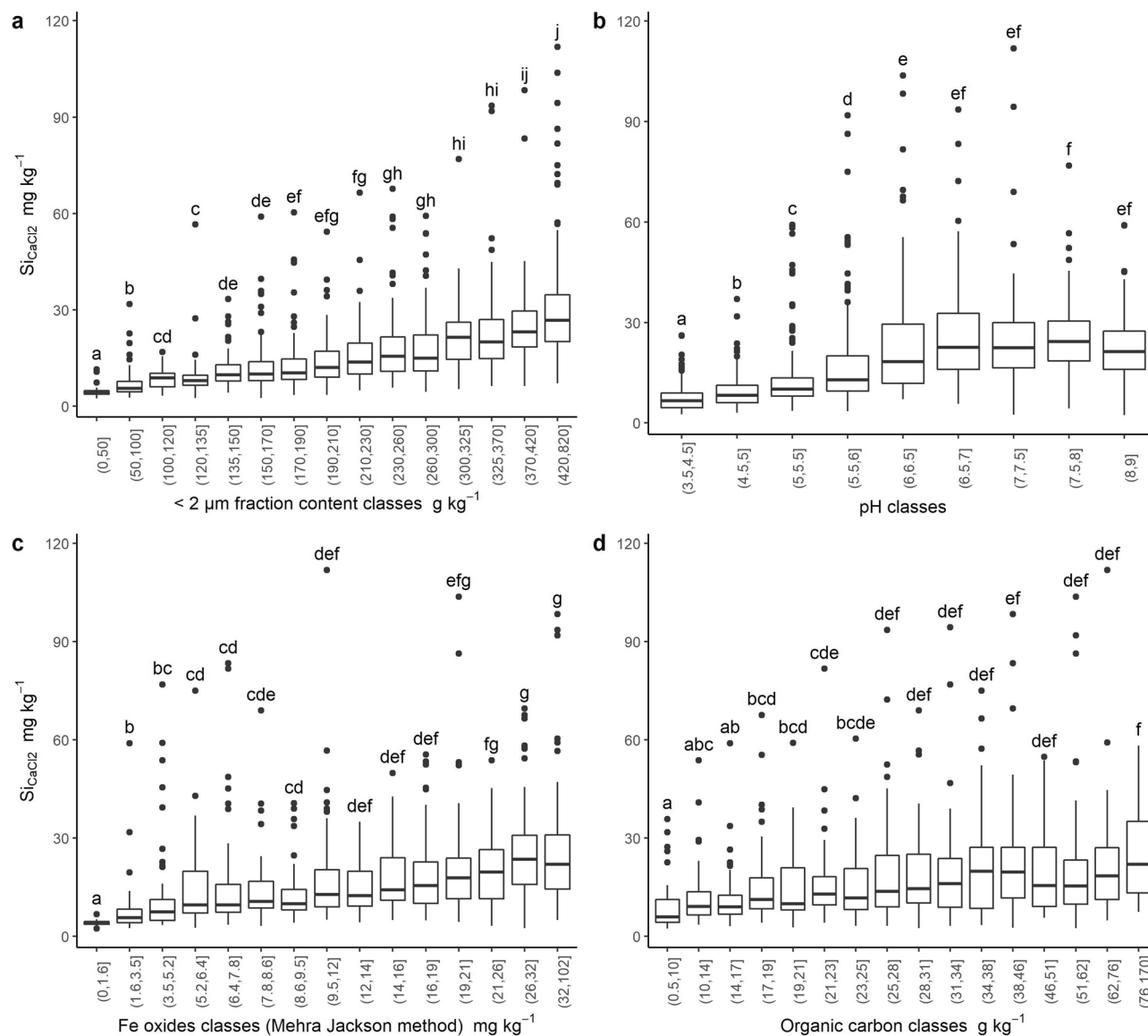


Figure 3. Boxplots of $\text{Si}_{\text{CaCl}_2}$ concentration as a function of (a) $< 2 \mu\text{m}$ fraction content classes, (b) pH classes, (c) Fe oxides concentration (estimated by the Mehra Jackson method) classes (d) soil organic carbon content classes for non-cultivated soils only. Classes have been created so that uncertainty around the central value does not overlap with the uncertainty around the central value of the surrounding classes. Classes with less than 40 individuals were merged. Groups of individuals sharing a letter are not significantly different according to pairwise comparisons of Wilcoxon test with Tukey adjustment for multiple comparisons.

shows that soil pH and clay nature were linked, with acidic soils being mainly kaolinitic and basic soils being more smectitic or rich in vermiculite. This could partially explain the link between $\text{Si}_{\text{CaCl}_2}$ concentration and pH, because kaolinites are more stable than other clay minerals (e.g. smectite)¹⁴.

For carbonated soils developed on sedimentary parent materials and podzols, the $\text{Si}_{\text{CaCl}_2}$ concentrations did not appear to be impacted by the nature of the corresponding clay mineral ($< 2 \mu\text{m}$ CEC) (Table 2). In carbonated soils on sediment parent material, the clay mineral assemblage was primarily dominated by smectite and vermiculite, according to the $< 2 \mu\text{m}$ CEC recorded (Fig. 4d). In podzols, the nature of the clay minerals did not vary much and primarily consisted of kaolinite and quartz in the $< 2 \mu\text{m}$ fraction (see the very low $< 2 \mu\text{m}$ CEC in Supplementary Table S2).

Our results showed that the increase in $\text{Si}_{\text{CaCl}_2}$ concentrations in tandem with pH may be explained by changes in the nature of the underlying mineralogy of the $< 2 \mu\text{m}$ fraction. In acidic soils with kaolinite as the primary clay component, the $\text{Si}_{\text{CaCl}_2}$ was lower than in soils with a near neutral pH, with a primary clay component of smectite.

Impact of agriculture on available silicon in soils. For soils derived from carbonated and non-carbonated sediment material (73% of French soils), $\text{Si}_{\text{CaCl}_2}$ significantly increased in the cultivated soils (perennial and annual crop) as compared to soils at uncultivated sites (Fig. 4a). Indeed, the results of linear model showed that

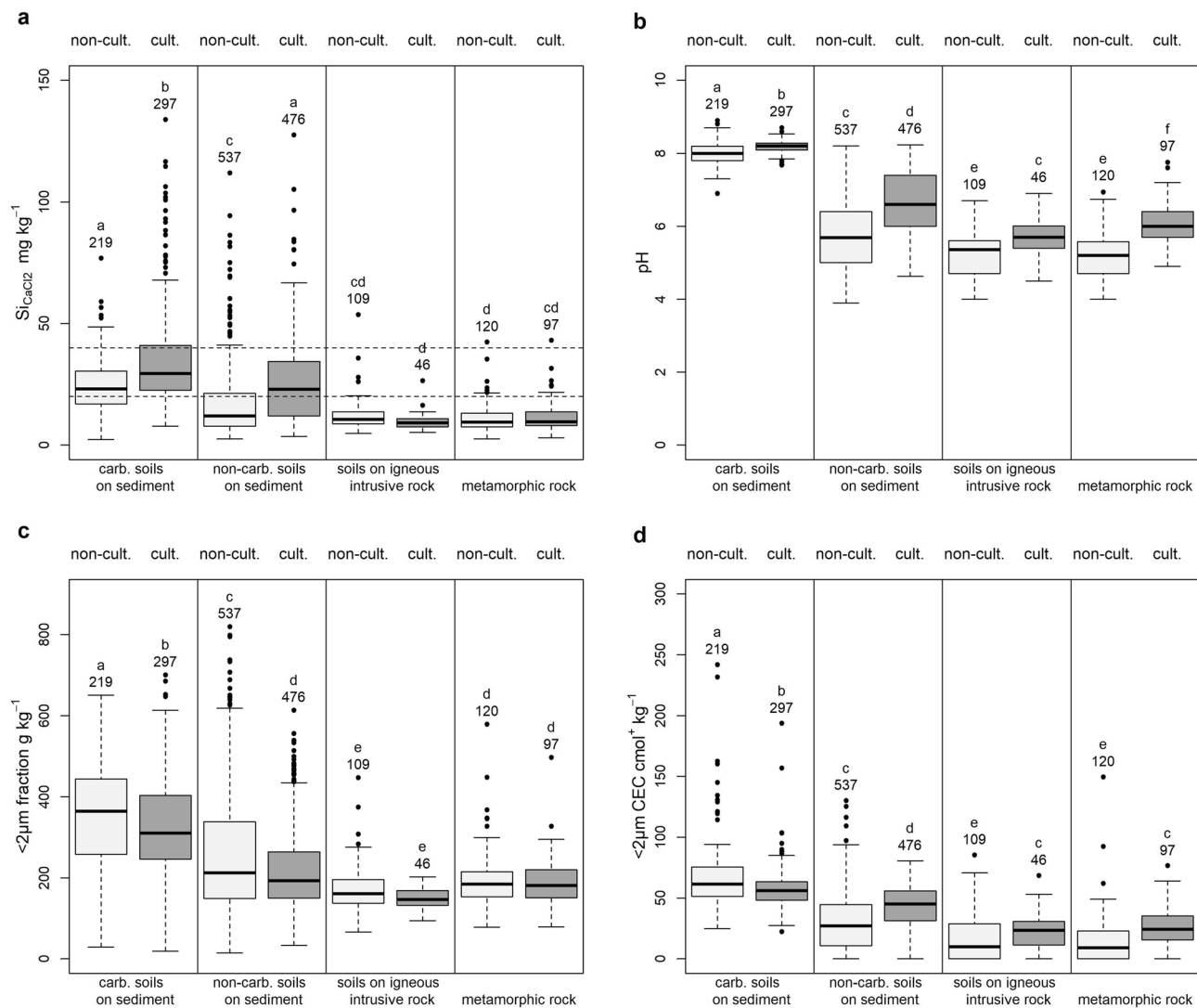


Figure 4. Boxplots by parent materials and land uses of: **(a)** $\text{Si}_{\text{CaCl}_2}$, **(b)** soil pH, **(c)** $<2\mu\text{m}$ fraction content, and **(d)** $<2\mu\text{m}$ CEC. Groups of individuals sharing a letter are not significantly different according to pairwise comparisons of Wilcoxon test with Tukey adjustment for multiple comparisons.

about 12% of the total variance is explained by this difference. However, for soils derived from igneous intrusive rock and metamorphic rock, there was no significant difference in $\text{Si}_{\text{CaCl}_2}$ concentrations between cultivated and non-cultivated sites. For these two parent materials, $\text{Si}_{\text{CaCl}_2}$ concentrations were very low, as compared to other parent materials. Thus contrarily to what was expected, cultivation increases $\text{Si}_{\text{CaCl}_2}$ concentrations but only in soils where this concentration is not too low.

Cultivated soils exhibited significantly higher pH values than uncultivated vegetated soils, regardless of parent material (Fig. 4b) due to liming practices on cultivation, with the notable exception of the carbonated soils, which are generally not limed. For carbonated soils, the difference of pH was due to acidifying conditions under non-cultivation, as compared to agricultural conditions. The difference in pH between cultivated and non-cultivated soils was less than 0.5 for carbonated soils on sediment and igneous intrusive rocks. Since carbonated soils have a $<2\mu\text{m}$ fraction content higher than 325 g kg^{-1} , pH has no effect on the $\text{Si}_{\text{CaCl}_2}$ concentration as shown by Fig. 5 and Table 2.

For non-carbonated soils on sediments and soils on metamorphic rocks, the difference was higher: the average pH of non-cultivated soils was 5.7 and 5.2, while the average pH of cultivated soils was 6.7 and 6.1 respectively for non-carbonated soils on sediments and metamorphic rocks (Supplementary Table S2).

As shown in Fig. 4c (and Supplementary Table S2), the $<2\mu\text{m}$ fractions for non-carbonated soils on sediments primarily comprised 50 to 325 g kg^{-1} . For this $<2\mu\text{m}$ fraction range, we showed that the $\text{Si}_{\text{CaCl}_2}$ concentration increased with pH (Fig. 5). Therefore, cultivation associated to a pH increase by liming may be responsible for the $\text{Si}_{\text{CaCl}_2}$ concentration increase under cultivation for these soils. This pH increase was also associated with an increase in $<2\mu\text{m}$ CEC and therefore with a higher smectite/vermiculite content under cultivation, and a higher illite/chorite content under permanent vegetation (Fig. 4d). Similar changes in clay mineral composition following changes in land use were observed on paired site approaches (Cornu et al.⁵⁴ and references herein).

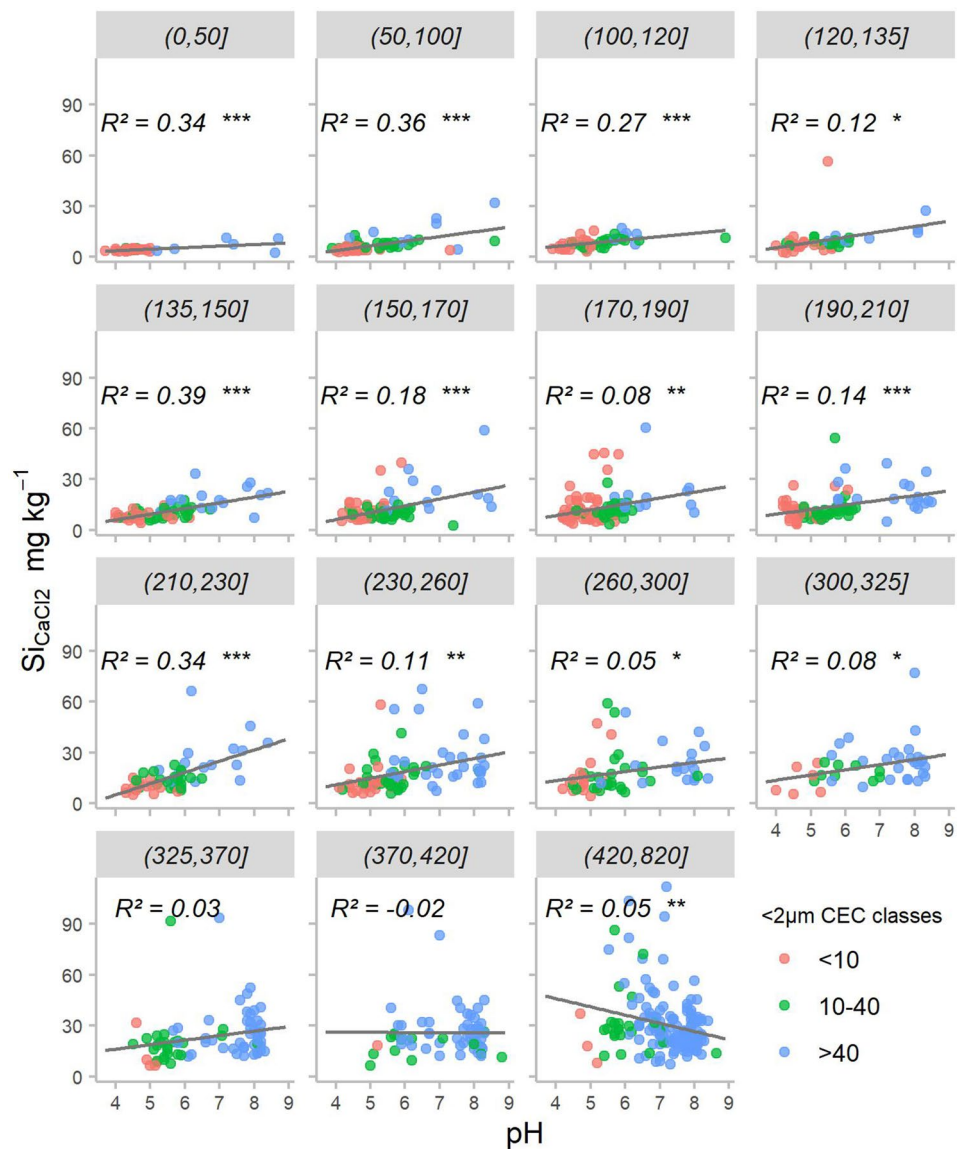


Figure 5. Relationship between topsoil $\text{Si}_{\text{CaCl}_2}$ and pH for the different $<2 \mu\text{m}$ content classes defined in Fig. 3, for non-cultivated soils. The classes of $<2 \mu\text{m}$ contents are expressed in g kg^{-1} and reported in the grey box at the top of the corresponding graph. The colours identify the classes of $<2 \mu\text{m}$ CEC corresponding to the classes of clay mineral CEC values provided by Goldberg et al.⁵³. Observations with $<2 \mu\text{m}$ CEC values larger than $100 \text{ cmol}^+ \text{ kg}^{-1}$ were eliminated (20 observations). Associated R^2 values and levels of significance are reported: ≤ 0.001 ‘***’, $[0.001; 0.01]$ ‘**’, $[0.01, 0.05]$ ‘*’, > 0.05 ‘.’.

The pH-driven effects of liming on $\text{Si}_{\text{CaCl}_2}$ concentrations have already been observed⁵². Indeed, increases in pH could cause higher adsorption of silicon to soil minerals and facilitate the solubilization of phytoliths in the soil solution, thus increasing the $\text{Si}_{\text{CaCl}_2}$ concentration at short time scales⁵².

Consequences in terms of potential PAS deficiency for wheat in temperate soils. To our knowledge, no study has defined the critical level of $\text{Si}_{\text{CaCl}_2}$ for avoiding Si deficiency for temperate staple crops as wheat. Critical levels are, however, available in the literature for rice and sugarcane; these levels are adopted as references for discussion here because wheat has a shoot Si concentration between those of rice and sugarcane¹⁰. We proposed two critical values: a lower bound (20 mg kg^{-1}) defined by Haysom and Chapman³³ for sugarcane in Australia, and an upper bound (40 mg kg^{-1}), an average value provided for rice based on data from silt loam in Louisiana soils³¹ (37 and 43 mg kg^{-1}) and from southern acidic soils in India³⁰ (43 mg kg^{-1}). We applied these two thresholds to the French soils cultivated with wheat, obtained by crossing the arable land pixels defined to Corine Land Cover map⁵⁵ with the cereal producing municipalities from the French OTEX classification (the Technico-economic orientation of the farms, <http://agreste.agriculture.gouv.fr>), to quantify the importance of potential $\text{Si}_{\text{CaCl}_2}$ deficiency in temperate soils (Fig. 2b). It results that only 4% of the soils cultivated with wheat fell below the 20 mg kg^{-1} critical level and could therefore be depleted of plant available Si. However, this hypoth-

esis requires a more technical definition of the Si requirements of wheat. Indeed, this would enable to determine if the soils having concentrations between 20 and 40 mg kg⁻¹ and representing 85% of the surfaces cultivated with wheat are below or under the critical level for wheat.

Materials and methods

Soil data from RMQS program. The soil data used in this study were provided by the French Soil Quality Monitoring Network (RMQS). The RMQS network consists of observation sites situated at the centre of a regular grid (16 × 16 km) covering the French territory. It provides 2111 sites in metropolitan France, almost half of which are cultivated (permanent crops or field crops) and the remaining of which consist of pastures, natural vegetation, or urban soils. The dataset used in this study corresponds to the first sampling campaign of the RMQS carried out from 2000 to 2009.

Soil type, parent material, climate, and land use were described in the field. At each site, 25 core samples were taken within a 20 m × 20 m plot and combined into a composite sample. Sampling depth generally consisted of the 0–30 cm layer⁴³. The composite samples were air-dried and sieved to 2 mm before being analysed in Soil Analysis Laboratory of INRAE (Arras, France).

The following parameters were measured: (i) the total soil organic carbon concentration, as measured by dry combustion (NF ISO 10694); (ii) the particle size distribution, by wet sieving and pipette method (NF X 31-107); (iii) cation exchange capacity (CEC) and exchangeable cations (cobaltihexamine method, NF X 31-130); (iv) pH in water (1 to 5 soil to water ratio, NF X 31-107); (v) calcium carbonate, using the volumetric method (NF X 31-106) (CaCO₃); and (vi) total P, K, Ca, Mg, Fe, and Al, determined by ICP-MS after dissolution with hydrofluoric and perchloric acids (NF X 31-147). The < 2 μm CEC was estimated as follows:

$$2 \mu\text{m CEC} = \frac{(CEC - 0.15 * OC)}{< 2 \mu\text{m fraction content}} * 1000 \quad (1)$$

with CEC in cmol⁺ kg⁻¹, OC in g kg⁻¹, and < 2 μm fraction content in g kg⁻¹. We used 0.15 cmol⁺ kg⁻¹ as an estimate of the CEC of organic matter.

Total Si was analysed from a subset of 673 samples by ICP after alkaline fusion⁵⁶, and extrapolated to the remaining sites using the following conceptual equation:

$$Si = f(Al, Fe, K, Na, Ca_{nc}, Mg_{nc}, P, SOC, CaCO_3, \text{residual water}) \quad (2)$$

where Ca_{nc} and Mg_{nc} are the fractions of Ca and Mg, respectively, that are not included in carbonate minerals or adsorbed to the exchangeable surfaces, and SOC is the organic carbon percentage. This model was implemented in cubist²⁹ and yielded an R² value greater than 0.98.

Bioavailable Si (Si_{CaCl2}) was estimated on samples from 2091 sites using the 0.01 M CaCl₂ method³³. This widely adopted method²⁵ allows estimation of the pool of readily soluble Si.

Bulk samples were equilibrated during 16 h at room temperature with 0.01 M CaCl₂ with a solid:liquid ratio of 1:10. Si was then analyzed, after filtration of the supernatant at 0.45 μm, by Inductively Coupled Plasma Atomic Emission Spectroscopy (axial ICP-AES; 720 ES, Varian)²⁹. The limit of quantification of the method was of 0.5 mg kg⁻¹ with an uncertainty, U, (with a confidence level of 0.95) evaluated as follow:

$$U = 0.0271 * Si_{CaCl2} + 0.25 \quad (3)$$

with Si_{CaCl2} and U expressed in mg kg⁻¹.

To decipher the impact of agricultural use on Si_{CaCl2} concentration, we stratified the database by (i) parent material, based on the European Soil Information System (EUSIS) classification⁵⁷ available at the French territory scale as in Landré et al.²⁹; and by (ii) land use. The group of soils developed on sediment was cut into two subgroups (carbonated and non-carbonated depending on their carbonate content (> 1% and < 1% respectively). We considered soils under forests, pastures, parks, natural vegetation, and wetlands to be non-cultivated soils. We did not make any distinction of land use for soils on igneous extrusive rocks (volcanic) and podzols, because cultivation of these soil types was limited to two and three sites, respectively.

Our statistical analysis was based on a subset of 1986 data points (*subset 1*, see Supplementary Table S1) due to the removal from the initial 2091 point dataset of any sites with missing geological information and three sites with peat soils.

Digital soil mapping approach. To map and define the spatial distribution of Si_{CaCl2} concentrations, we implemented a digital soil mapping (DSM) approach based on the *scorpan* model framework proposed by McBratney et al.⁵⁸, a spatial prediction function utilizing quantitative relationships between soil properties and soil forming factors as follows:

$$Soil_x = f(s, c, o, r, p, a, n) + e \quad (4)$$

where *Soil* is a soil property at position *x*. The *s* refers to soil information derived from prior soil maps or from remote or proximal sensing data; *c* refers to the climatic properties of the environment at a given point; *o* refers to organisms, including vegetation, fauna, or human activity; *r* refers to relief; *p* refers to the parent material or lithology; *a* refers to the soil age; *n* refers to space or spatial position; and *e* is the spatially correlated errors.

To apply this model, we retained a set of spatial covariates describing *scorpan* factors to predict the spatial distribution of Si_{CaCl2} at 90 m resolution. All covariates were previously resampled at the same resolution. The selection was carried out from a larger set of covariates using a combination of expert knowledge and statistical

approaches. The latter was based on the *boruta* package in R⁵⁹. This algorithm uses the classification of the covariate importance implemented in the *randomForest* package and compares the importance with random variables based on the Z score value. This step allows the identification of the most relevant covariates before fitting a prediction model. The initial 18 spatial covariates represented the *scorpan* factors as follows: *soil* (map of soil type and available water capacity (AWC)), *climate* (map of climate type, precipitation, and evapotranspiration), *vegetation* (land use, forest type), *parent material* (parent material types and gravimetry), and *relief* (shuttle radar topography mission (SRTM), compound topographic index (CTI), slope cosine, erosion, slope, and slope position). A final covariate corresponding to the normalized difference vegetation index (NDVI) was derived from remote sensing data. This spectral index is widely used to describe the photosynthetic capacity of vegetative cover. The underlying assumption driving this method holds that changes in vegetation may reflect various plant responses to climate, land management, or soil properties⁴⁷. This covariate was computed from a large time series dataset. To summarise the temporal data, Loiseau et al.⁴⁷ performed a principal component analysis that yielded 3 covariates corresponding to the 3 first components: NDVI_1, NDVI_2, and NDVI_3.

For the *scorpan* model, we developed a regression kriging (RK) model using the selected covariates and soil observations. The RK model is a hybrid technique combining a Random Forest approach with a geostatistical approach. Random Forest⁶⁰ consists of an ensemble of regression trees built from covariates and point data. The final prediction is the mean of the individual tree predictions. This technique is applicable in R and requires two main parameters: the number of randomly selected splitting variables at each tree (*mtry*), and the number of trees (*ntree*). We used the default parameters provided by the package (*mtry* = 6 and *ntree* = 500). The final predictions are the sum of the Random Forest predictions and the residuals computed through an ordinary kriging procedure⁶¹.

The RK model was fitted on the on a subset of the RMQS sites for which covariate information were available (*subset 2*: 1987 points, see Supplementary Table S1). This procedure was implemented with the package *GSIF*⁶², which also allows fitting of residuals in a variogram.

To assess the covariates importance in the model, we used the function *varImp()* implemented in the *Random Forest* package. The function calculates the difference in MSE (Mean Squared Error) when the values of each predictor are shuffled. This indicator is then normalized by the standard deviation of the differences to obtain the Increase in MSE noted %IncMSE. The highest values are attributed to the more important variables.

The validity of the fitted prediction model was evaluated by a 30-fold cross validation. At each step, the soil dataset was split into two datasets: 2/3 for calibration, and 1/3 for validation.

To obtain an estimate of the final map accuracy, the validation indicators were calculated at each iteration and then averaged over the 30 repetitions. We used different indicators for validation, including the Root Mean Square Error (RMSE), the coefficient of determination (R^2), the concordance⁶³, and the bias.

Take home messages. The $\text{Si}_{\text{CaCl}_2}$ concentrations in French soils is highly variable (from 2.3 to 134 mg kg⁻¹) and depends mainly on parent material and soil type, but also on the land use.

When the soils are cultivated, the concentration in $\text{Si}_{\text{CaCl}_2}$ significantly increases for soils developed on sediment parent material but not for those developed on metamorphic rocks and igneous intrusive rocks. For these two last parent materials, $\text{Si}_{\text{CaCl}_2}$ concentration is low compared to soils developed on sediments. For soil developed on igneous extrusive rocks and podzol, no conclusion on the impact of agriculture on $\text{Si}_{\text{CaCl}_2}$ concentrations could be drawn due to the low number of sites under cultivation for these soils in France. For non-carbonated soils, this increase is due to the pH increase associated to liming practices. More research is needed to better understand the impact of cultivation on $\text{Si}_{\text{CaCl}_2}$ concentration for carbonated soils for example through a paired sites approach.

We also verified on this large panel of temperate soils that the $\text{Si}_{\text{CaCl}_2}$ concentration is governed by the < 2 μm fraction, pH, and iron oxide content to a lesser extent. The nature of the clay assemblage seemed also to act on the $\text{Si}_{\text{CaCl}_2}$ concentration. We however showed that the $\text{Si}_{\text{CaCl}_2}$ concentration increases with pH only for soils with content in < 2 μm fraction ranging from 50 to 325 g kg⁻¹.

We also showed that 4% of the soils cropped with wheat could be deficient in $\text{Si}_{\text{CaCl}_2}$. This result was based on critical level of $\text{Si}_{\text{CaCl}_2}$ estimated for sugar cane and rice. Studies should be done to determine precisely the critical level for wheat.

At last, this study did not allow accessing the kinetic aspects. Other Si pools and/or chronosequences studies should be analyzed to answer this question.

Data availability

The dataset analysed during the current study can be retrieved from <https://doi.org/10.15454/CFWBAA>⁶⁴. However, the location information is not publicly accessible because the data contain confidential information.

Received: 6 April 2020; Accepted: 15 October 2020

Published online: 17 November 2020

References

1. Coskun, D. et al. The controversies of silicon's role in plant biology. *New Phytol.* **221**, 67–85 (2019).
2. Datnoff, L. E., Snyder, G. H. & Korndörfer, G. H. *Silicon in Agriculture* (Elsevier, Amsterdam, 2001).
3. Epstein, E. The anomaly of silicon in plant biology. *Proc. Natl. Acad. Sci.* **91**, 11–17 (1994).
4. Liang, Y., Sun, W., Zhu, Y.-G. & Christie, P. Mechanisms of silicon-mediated alleviation of abiotic stresses in higher plants: A review. *Environ. Pollut.* **147**, 422–428 (2007).
5. Meunier, J. D. et al. Effect of phytoliths for mitigating water stress in durum wheat. *New Phytol.* **215**, 229–239 (2017).
6. Exley, C. & Guerriero, G. A reappraisal of biological silicification in plants?. *New Phytol.* **223**, 511–513 (2019).

7. Liang, Y., Nikolic, M., Bélanger, R., Gong, H. & Song, A. *Silicon in Agriculture* (Springer, Dordrecht, 2015). <https://doi.org/10.1007/978-94-017-9978-2>.
8. Guntzer, F., Keller, C. & Meunier, J.-D. Benefits of plant silicon for crops: A review. *Agron. Sustain. Dev.* **32**, 201–213 (2012).
9. Katz, O. Silica phytoliths in angiosperms: Phylogeny and early evolutionary history. *New Phytol.* **208**, 642–646 (2015).
10. Hodson, M. J., White, P. J., Mead, A. & Broadley, M. R. Phylogenetic variation in the silicon composition of plants. *Ann. Bot.* **96**, 1027–1046 (2005).
11. Darmawan, *et al.* Effect of long-term intensive rice cultivation on the available silica content of sawah soils: Java Island, Indonesia. *Soil Sci. Plant Nutr.* **52**, 745–753 (2006).
12. Savant, N. K., Datnoff, L. E. & Snyder, G. H. Depletion of plant-available silicon in soils: A possible cause of declining rice yields. *Commun. Soil Sci. Plant Anal.* **28**, 1245–1252 (1997).
13. Yan, G., Nikolic, M., Ye, M., Xiao, Z. & Liang, Y. Silicon acquisition and accumulation in plant and its significance for agriculture. *J. Integr. Agric.* **17**, 2138–2150 (2018).
14. Cornelis, J.-T. & Delvaux, B. Soil processes drive the biological silicon feedback loop. *Funct. Ecol.* **30**, 1298–1310 (2016).
15. Alexandre, A., Meunier, J.-D., Colin, F. & Koud, J.-M. Plant impact on the biogeochemical cycle of silicon and related weathering processes. *Geochim. Cosmochim. Acta* **61**, 677–682 (1997).
16. Derry, L. A., Kurtz, A. C., Ziegler, K. & Chadwick, O. A. Biological control of terrestrial silica cycling and export fluxes to watersheds. *Nature* **433**, 728–731 (2005).
17. Berner, E. K. & Berner, R. A. *Global Environment: Water, Air and Geochemical Cycles* (Prentice Hall, Old Tappan, 1996).
18. Brantley, S. L. Reaction kinetics of primary rock-forming minerals under ambient conditions. In *Treatise on Geochemistry*, Vol. 5 (Elsevier, Amsterdam, 2005).
19. Riotte, J. *et al.* Processes controlling silicon isotopic fractionation in a forested tropical watershed: Mule Hole Critical Zone Observatory (Southern India). *Geochim. Cosmochim. Acta* **228**, 301–319 (2018).
20. Puppe, D., Kaczorek, D., Wanner, M. & Sommer, M. Dynamics and drivers of the protozoic Si pool along a 10-year chronosequence of initial ecosystem states. *Ecol. Eng.* **70**, 477–482 (2014).
21. Hiemstra, T., Barnett, M. O. & van Riemsdijk, W. H. Interaction of silicic acid with goethite. *J. Colloid Interface Sci.* **310**, 8–17 (2007).
22. Sauer, D., Saccone, L., Conley, D. J., Herrmann, L. & Sommer, M. Review of methodologies for extracting plant-available and amorphous Si from soils and aquatic sediments. *Biogeochemistry* **80**, 89–108 (2006).
23. Tubaña, B. S. & Heckman, J. R. Silicon in soils and plants. In *Silicon and Plant Diseases* (eds Rodrigues, F. A. & Datnoff, L. E.) (Springer International Publishing, Berlin, 2015). https://doi.org/10.1007/978-3-319-22930-0_2.
24. Li, Z. *et al.* Combined silicon-phosphorus fertilization affects the biomass and phytolith stock of rice plants. *Front. Plant Sci.* **11**, 67 (2020).
25. Meunier, J.-D., Sandhya, K., Prakash, N. B., Borschneck, D. & Dussouillez, P. pH as a proxy for estimating plant-available Si? A case study in rice fields in Karnataka (South India). *Plant Soil* **432**, 143–155 (2018).
26. Miles, N., Manson, A. D., Rhodes, R., van Antwerpen, R. & Weigel, A. Extractable silicon in soils of the South African sugar industry and relationships with crop uptake. *Commun. Soil Sci. Plant Anal.* **45**, 2949–2958 (2014).
27. Phonde, D. B., Deshmukh, P. S., Banerjee, K. & Adsule, P. G. Plant available silicon in sugarcane soils and its relationship with soil properties, leaf silicon and cane yield. *Asian J. Soil Sci.* **9**, 176–180 (2014).
28. Yanai, J., Taniguchi, H. & Nakao, A. Evaluation of available silicon content and its determining factors of agricultural soils in Japan. *Soil Sci. Plant Nutr.* **62**, 511–518 (2016).
29. Landré, A. *et al.* Do climate and land use affect the pool of total silicon concentration? A digital soil mapping approach of French topsoils. *Geoderma* **364**, 114175 (2020).
30. Narayanaswamy, C. & Nagabovanalli, P. Calibration and categorization of plant available silicon in rice soils of South India. *J. Plant Nutr.* **32**, 1237–1254 (2009).
31. Babu, T., Tubana, B., Paye, W., Kanke, Y. & Datnoff, L. Establishing soil silicon test procedure and critical silicon level for rice in Louisiana soils. *Commun. Soil Sci. Plant Anal.* <https://doi.org/10.1080/00103624.2016.1194996> (2016).
32. Korndörfer, G., Snyder, G., Ulloa, M., Powell, G. & Datnoff, L. Calibration of soil and plant silicon analysis for rice production. *J. Plant Nutr.* **24**(7), 1071–1084 (2006).
33. Haysom, M. B. C. & Chapman, L. S. Some aspects of the calcium silicate trials at Mackay. *Proc. Queens. Soc. Sugar Cane Technol.* **42**, 117–122 (1975).
34. Clymans, W., Struyf, E., Govers, G., Vandevenne, F. & Conley, D. J. Anthropogenic impact on amorphous silica pools in temperate soils. *Biogeosciences* **8**, 2281–2293 (2011).
35. Datnoff, L. & Rodrigues, F. The role of silicon in suppressing rice diseases. *APSnet Features* **58** (2005).
36. Desplanques, V. *et al.* Silicon transfers in a rice field in Camargue (France). *J. Geochem. Explor.* **88**, 190–193 (2006).
37. Eneji, E. *et al.* Effect of calcium silicate on growth and dry matter yield of *Chloris gayana* and *Sorghum sudanense* under two soil water regimes. *Grass Forage Sci.* **60**, 393–398 (2005).
38. Meunier, J. D., Guntzer, F., Kirman, S. & Keller, C. Terrestrial plant-Si and environmental changes. *Mineral. Mag.* **72**, 263–267 (2008).
39. Guntzer, F., Keller, C., Poulton, P. R., McGrath, S. P. & Meunier, J.-D. Long-term removal of wheat straw decreases soil amorphous silica at Broadbalk, Rothamsted. *Plant Soil* **352**, 173–184 (2012).
40. Watanabe, T., Luu, H. M., Nguyen, N. H., Ito, O. & Inubushi, K. Combined effects of the continual application of composted rice straw and chemical fertilizer on rice yield under a double rice cropping system in the Mekong Delta, Vietnam. *Jpn. Agric. Res. Q.* **47**, 397–404 (2013).
41. Barão, L. *et al.* Silicon mobilization in soils: the broader impact of land use. *Silicon* **12**, 1529–1538 (2020).
42. Minasny, B., Mcbratney, A. & Hartemink, A. Global pedodiversity, taxonomic distance, and the World Reference Base. *Geoderma* **155**, 132–139 (2010).
43. Jolivet, C., Boulonne, L. & Ratié, C. Manuel du Réseau de Mesures de la Qualité des Sols. (2006).
44. Mulder, V. L., Lacoste, M., Richer-de-Forges, A. C. & Arrouays, D. GlobalSoilMap France: High-resolution spatial modelling the soils of France up to two meter depth. *Sci. Total Environ.* **573**, 1352–1369 (2016).
45. Adhikari, K. *et al.* High-resolution 3-D mapping of soil texture in Denmark. *Soil Sci. Soc. Am. J.* **77**, 860–876 (2013).
46. Padarian, J., Minasny, B. & Mcbratney, A. B. Chile and the Chilean soil grid: A contribution to GlobalSoilMap. *Geoderma Reg.* **9**, 17–28 (2017).
47. Loiseau, T. *et al.* Satellite data integration for soil clay content modelling at a national scale. *Int. J. Appl. Earth Obs. Geoinf.* **82**, 101905 (2019).
48. Mehra, O. P. & Jackson, M. L. Iron oxide removal from soils and clays by a dithionite-citrate system buffered with sodium bicarbonate. *Clays Clay Miner.* **7**, 317–327 (1960).
49. Kaczorek, D., Puppe, D., Busse, J. & Sommer, M. Effects of phytolith distribution and characteristics on extractable silicon fractions in soils under different vegetation—An exploratory study on loess. *Geoderma* **356**, 113917 (2019).
50. Irfan, K. Impact of 60 years of intensive rice cropping on clay minerals in soils due to Si exportation. *Am. J. Agric. For.* **5**, 40 (2017).
51. Nguyen, M. N. *et al.* Silicic acid as a dispersibility enhancer in a Fe-oxide-rich kaolinitic soil clay. *Geoderma* **286**, 8–14 (2017).
52. Haynes, R. J. What effect does liming have on silicon availability in agricultural soils?. *Geoderma* **337**, 375–383 (2019).

53. Goldberg, S., Lebron, I., Seaman, J. C. & Suarez, D. L. Soil colloidal behaviour. In *Handbook of Soil Sciences* (CRC, Taylor & Francis [distributor], Boca Raton, 2011).
54. Cornu, S., Montagne, D., Hubert, F., Barré, P. & Caner, L. Evidence of short-term clay evolution in soils under human impact. *C. R. Geosci.* **344**, 747–757 (2012).
55. European Environment Agency. *CLC2006 Technical Guidelines*. (2007).
56. Landré, A. *et al.* Prediction of total silicon concentrations in French soils using pedotransfer functions from mid-infrared spectrum and pedological attributes. *Geoderma* **331**, 70–80 (2018).
57. King, D., Daroussin, J. & Tavernier, R. Development of a soil geographic database from the Soil Map of the European Communities. *CATENA* **21**, 37–56 (1994).
58. McBratney, A. B., Mendonça Santos, M. L. & Minasny, B. On digital soil mapping. *Geoderma* **117**, 3–52 (2003).
59. Kursu, M. B. & Rudnicki, W. R. Feature selection with the Boruta package. *J. Stat. Softw.* **36**, 1–3 (2010).
60. Breiman, L. Random Forests. *Mach. Learn.* **45**, 5–32 (2001).
61. Keskin, H. & Grunwald, S. Regression kriging as a workhorse in the digital soil mapper's toolbox. *Geoderma* **326**, 22–41 (2018).
62. Hengl, T., Kempen, B., Heuvelink, G. B. M. & Malone, B. P. GSIF: Global Soil Information Facilities. (2019).
63. Lin, L. I. K. A concordance correlation coefficient to evaluate reproducibility. *Biometrics* **45**, 255–268 (1989).
64. Saby, N. P. A. *et al.* Données de réplication pour : Agriculture increases the bioavailability of silicon, a beneficial element for crop, in temperate soils. <https://doi.org/10.15454/CFWBAA> (2020).

Acknowledgements

This work was performed in the frame of the French ANR BioSiSol project (ANR-14-CE01-0002). RMQS soil sampling and physico-chemical analyses were supported by the GIS Sol, which is a scientific group of interest on soils involving the French Ministry for ecology and sustainable development and Ministry of agriculture, the French National forest inventory (IFN), ADEME, IRD and INRAE. The authors are grateful to Annie Guérin (LAS, INRAE, Arras, France) and Amélia Landré (INFOSOL, INRAE, Orléans, France) for Si_{CaCl2} analysis and database preparation respectively.

Author contributions

M.C. performed the data treatment and statistical analyses and contributed to the writing of the manuscript. N.S. contributed to the writing of the proposal, supervised M.C. in the data treatment methods and analysis, and contributed to the writing. S.C. and J.D.M. wrote the proposal and contributed to the interpretation of the data and to the manuscript writing.

Competing interests

The authors declare no competing interests.

Additional information

Supplementary information is available for this paper at <https://doi.org/10.1038/s41598-020-77059-1>.

Correspondence and requests for materials should be addressed to S.C.

Reprints and permissions information is available at www.nature.com/reprints.

Publisher's note Springer Nature remains neutral with regard to jurisdictional claims in published maps and institutional affiliations.



Open Access This article is licensed under a Creative Commons Attribution 4.0 International License, which permits use, sharing, adaptation, distribution and reproduction in any medium or format, as long as you give appropriate credit to the original author(s) and the source, provide a link to the Creative Commons licence, and indicate if changes were made. The images or other third party material in this article are included in the article's Creative Commons licence, unless indicated otherwise in a credit line to the material. If material is not included in the article's Creative Commons licence and your intended use is not permitted by statutory regulation or exceeds the permitted use, you will need to obtain permission directly from the copyright holder. To view a copy of this licence, visit <http://creativecommons.org/licenses/by/4.0/>.

© The Author(s) 2020